Self-similar spatiotemporal solitary waves in Bessel–Hermite optical lattices*

Xu Si-Liu(徐四六)[a], Liang Jian-Chu(梁检初)[b], and Li Zhong-Ming(李忠明)[a]†

[a] School of Electronics and Information Engineering, Xianning University, Xianning 437100, China
[b] Department of Electronic Science, Huizhou University, Huizhou 516001, China

(Received 21 April 2011; revised manuscript received 3 June 2011)

An exact self-similar solution to a (3+1)-dimensional nonlinear Schrödinger equation with gain in the Bessel–Hermite lattice is obtained analytically. The stability of the analytical solution is confirmed by using numerical simulation. It is shown that the light bullet has a stable ellipsoid or vortex profile and a linear spatiotemporal chirp.

Keywords: spatiotemporal solitons, self-similar technology

PACS: 42.65.Tg, 42.81.Dp **DOI:** 10.1088/1674-1056/20/11/114214

1. Introduction

Optical spatiotemporal solitons (also known as light bullets), which were first proposed by Silberberg,[1] have attracted a lot of attention.[2−4] There are a set of important theoretical and experimental investigations on spatiotemporal solitons in self-focusing and defocusing nonlinear media.[5] In general, the existence of the light bullets (LBs) results from the simultaneous balance of the medium nonlinearity against the diffraction and dispersion. In this regard, the nonlinear self-similar propagation is a behaviour without collapse at high power.[6−8] The self-similar behaviour is related to a featuring beam or a pulse profile that holds the same shape during the propagation (evolution). Up to now, a few self-similar nonlinear waves have been studied in nonlinear optics.[7−8] Correlative researches have been reported in higher dimensions, including the self-similar beam collapse,[9,10] the two-dimensional (2D) beam propagation,[11] and the self-similar soliton solutions in graded index media.[12]

It is known that multi-dimensional solitons in Kerr-type focusing media are unstable against collapse, hence the search for suitable media for the creation of stable three-dimensional (3D) LBs remains an interesting topic.[13] The same problem encumbers the creation of multi-dimensional solitons in self-attractive Bose–Einstein condensates. Various schemes to stabilize solitons in cubic media have been proposed.[14,15] Stable ring shape solitons in cylindrical lattices are also discussed in media with the saturable nonlinearity of the photo-refractive type.[16] The spatial modulation of the refractive index profoundly affects the soliton properties.[17−19] In photo-refractive materials,[20] optical lattices with tunable refractive-index modulation depth and period can be induced optically. As mentioned above, many efforts have been devoted to the investigation of solitons supported by lattices with a honeycomb symmetry.[20,21] In contrast to the extended shape of the honeycomb lattices, the Bessel lattice provides a new kind of localized refractive-index modulation. The Bessel lattice has a good prospect for waveguide because of the following two aspects. Firstly, as eigenmode solutions of the linear Schrödinger equation, the Bessel beams can propagate in the free space without diffraction and the Bessel lattice can be induced by the non-diffracting Bessel beams created in experiments with a conical prism (axicon)[22] or a computer-generated hologram.[23] Secondly, differing from the square periodic lattice, the Bessel lattice is bound lattice with energy centralized in the internal layers. So the Bessel lattice becomes an important concentric optical photonic lattice supporting lattice solitons and has attracted much attention.[24−27] It is possible to produce the Bessel lattice with a radial shape.[24,28] Such a lattice is especially interesting because of the suppressed diffraction of the lattice-inducing field, which is sim-

*Project supported by the National Basic Research Program of China (Grant No. 2009CB921605).
†Corresponding author. E-mail: Lzhming001@163.com
© 2011 Chinese Physical Society and IOP Publishing Ltd

ilar to that in the case of the harmonic lattice.[29] In 2005, Mihalache *et al.*[28] constructed families of 3D spatiotemporal solitons supported by the zeroth order Bessel optical lattices, which is the first example of a 3D soliton stabilized by an axially symmetric lattice. To the best of our knowledge, it has not yet been reported that 3D self-similar spatiotemporal solitons can be stabilized by the higher-order Bessel–Hermite (BH) lattices.

The system under our consideration is described by a (3+1)-D nonlinear Schrödinger equation (NLSE) with gain in the BH lattice. Exact self-similar spatiotemporal soliton clusters are obtained. We show that these solitons with various modes can be classed with the LB family. The present BH lattice is imprinted in a de-focusing cubic nonlinear medium, and the lattice is both time- and space-dependent.

The rest of the present paper is organized as follows. After the proposal of the (3+1)-D NLSE with gain in an external lattice potential, the exact self-similar solution is deduced analytically in Section 2. The numeric simulation and the discussion are presented in Section 3. Finally, the concluding remarks and conclusion are given in Section 4.

2. Model and exact self-similar solution

The (3+1)-D NLSE with gain in an optical lattice potential can be expressed as[3,30]

$$\begin{aligned} \mathrm{i}\,\psi_z \,=\, & -\frac{1}{2k}\boldsymbol{\nabla}_\perp^2\psi+\frac{\beta_2}{2}\psi_{\tau\tau}-\frac{kn_2}{n_0}\left|\psi\right|^2\psi \\ & +M\left(z,x,y,\tau\right)\psi+\mathrm{i}\,\frac{g\left(z\right)}{2}\psi, \end{aligned} \tag{1}$$

where $\psi(z,x,y,\tau)$ is the spatiotemporal field envelope propagating along z, τ is the comoving time, $\boldsymbol{\nabla}_\perp$ is the transverse Laplacian acting on (x,y), β_2 is the group-velocity dispersion, kn_2/n_0 accounts for the Kerr nonlinearity, $g(z)$ is the distributed gain, $k=(2\pi/\lambda)n_0$ is the wave number in the medium, n_0 and n_2 are the linear and the nonlinear refractive indices, respectively, and $M(z,x,y,\tau)$ is the optical lattice potential, which is both time- and space-dependent. We assume that the refractive index modulation is induced by the multiple incoherent nonzero-order BH beams. In this case, $M(z,x,y,\tau)$ measures the local modulation of the refractive index for the probe signal, which is induced by the pump beam through the cross-phase modulation.[31] Hence here this choice of the optical lattice potential implies the interference between the BH beam and a stronger plane wave. The pump beam is assumed to propagate in a nearly linear regime, which actually implies the strong saturation of the pump beam in the medium with a saturable nonlinearity.

We consider the defocusing nonlinearity ($n_2<0$) and the anomalous dispersion ($\beta_2<0$), a combination of which is accessible in novel (e.g., quadratic) nonlinear materials.[29] With the introduction of normalized variables $Z=z/L$, $X=x/w_0$, $Y=y/w_0$, $T=\tau/\left(L\left|\beta_2\right|\right)^{1/2}$, $G(z)=gL$, and $\Psi=\left(k\left|n_2\right|L/n_0\right)^{1/2}\psi$, the resultant normalized propagation equation is

$$\begin{aligned} \mathrm{i}\,\Psi_Z \,=\, & -\frac{1}{2}\boldsymbol{\nabla}^2\Psi+\left|\Psi\right|^2\Psi+\mathrm{K}\left(Z,X,Y,T\right)\Psi \\ & +\mathrm{i}\,\frac{G\left(Z\right)}{2}\Psi, \end{aligned} \tag{2}$$

where

$$\boldsymbol{\nabla}^2=\frac{\partial^2}{\partial X^2}+\frac{\partial^2}{\partial Y^2}+\frac{\partial^2}{\partial T^2}$$

is the spatiotemporal Laplacian, w_0 is the characteristic transverse width, $L=kw_0^2$ is the diffraction length, and $K=LM$ is the optical lattice potential.

To find the self-similar solution of Eq. (2), we first write the field in the cylindrical coordinates as $\Psi\left(Z,R,\phi,T\right)=A\left(Z,R,\phi,T\right)\mathrm{e}^{\mathrm{i}\,\Phi(Z,R,T)}$, where $R=\sqrt{X^2+Y^2}$ is the spatial radius, and φ is the azimuthal angle in transverse plane (X,Y). The amplitude $A\left(Z,R,\phi,T\right)=E(Z)\varphi\left(\phi\right)\Pi\left(T\right)F\left(\theta\right)/(-2Z)$ and the phase $\Phi\left(Z,R,T\right)=a\left(Z,T\right)+c\left(Z,T\right)R^2$ are real functions. Here $E\left(Z\right)=E_0\exp\left[\int_0^Z G\left(Z'\right)\mathrm{d}Z'\right]$ is the normalized energy variable, which relates to the energy in real physical units through a multiplication factor $n_0\sqrt{L\left|\beta_2\right|}/k^2\left|n_2\right|$, $\theta\left(Z,R\right)=R/(-2Z)$ is the self-similar variable, $a\left(Z,T\right)$ is the phase offset, and $c\left(Z,T\right)$ represents the wave front curvature. Substituting $\Psi(Z,R,\phi,T)$ into Eq. (2) and requiring that the real and the imaginary parts of each term be separately equal to zero, we obtain $c\left(Z,T\right)=c_0/(1-2c_0Z)$ and

$$\begin{aligned} & \theta^2\frac{\mathrm{d}^2F\left(\theta\right)}{\mathrm{d}\theta^2}+\theta\frac{\mathrm{d}F\left(\theta\right)}{\mathrm{d}\theta}+\left[2\left(1-2Z\right)^2\frac{\mathrm{d}a}{\mathrm{d}Z}\theta^2\right. \\ & \left.+\frac{1}{\phi\left(\varphi\right)}\frac{\mathrm{d}^2\phi\left(\varphi\right)}{\mathrm{d}\varphi^2}+\frac{\left(1-2Z\right)^2}{\Pi}\frac{\mathrm{d}^2\Pi}{\mathrm{d}T^2}\theta^2\right]F\left(\theta\right) \\ & -2\left[\theta^2\left|F\left(\theta\right)\phi\left(\varphi\right)\Pi\left(T\right)\right|^2\,\mathrm{e}^{\int_0^Z G(z')\,\mathrm{d}z'}\right. \\ & \left.-R^2K\left(Z,R,\varphi,T\right)\right]F\left(\theta\right)=0. \end{aligned} \tag{3}$$

According to the principle of separation of variables, it can be further deduced that

$$\frac{1}{\varphi(\phi)}\frac{\mathrm{d}^2\varphi(\phi)}{\mathrm{d}\phi^2} = -m^2, \tag{4}$$

$$\frac{1}{\Pi(T)}\frac{\mathrm{d}^2\Pi(T)}{\mathrm{d}^2T} - T^2 = -n, \tag{5}$$

$$2(1-2Z)^2\frac{\mathrm{d}a}{\mathrm{d}Z} + (T^2-n)(1-2Z)^2 = \lambda^2. \tag{6}$$

The solutions for Eqs. (4), (5) and (6) are

$$\varphi_m(\phi) = \frac{1}{\sqrt{1+q^2}}\left[\cos(m\phi) + \mathrm{i}\,q\sin(m\phi)\right], \tag{7}$$

$$\Pi_n(T) = N_n\,\mathrm{e}^{-\frac{T^2}{2}}\mathrm{H}_n(T), \tag{8}$$

$$a(Z,T) = a_0 + \frac{n-T^2}{2}Z + \frac{\lambda^2}{4(1-2Z)}, \tag{9}$$

where $\mathrm{H}_n(T) = (-1)^n\,\mathrm{e}^{T^2}\mathrm{d}^n\,\mathrm{e}^{-T^2}/\mathrm{d}T^n$ is the Hermite polynomial, $N_n = \left(1/\sqrt{\pi}2^n n!\right)^{1/2}$ is the normalization constant, integers m $(=0,\pm1,\pm2,\ldots)$ and $n\,(=0,\pm1,\pm2,\ldots)$ denote the quantum numbers of φ and Π, respectively, λ is a constant that is to be determined, phase offset a_0 and chirp parameter c_0 are the integration constants depending on the initial conditions of the wave packet, real number q is the so-called azimuthal modulation depth: $q=1$ corresponds to an azimuthally homogeneous solution and $q=0$ means the total modulation in the azimuthal direction. Inserting Eqs. (4), (5), and (6) into Eq. (3), we have

$$\theta^2\frac{\mathrm{d}^2F(\theta)}{\mathrm{d}\theta^2} + \theta\frac{\mathrm{d}F(\theta)}{\mathrm{d}\theta} + \left(\lambda^2\theta^2 - m^2\right)F(\theta) - 2\Big[\theta^2\left|F(\theta)\,\phi_m(\varphi)\,\Pi_n(T)\right|^2 \times \mathrm{e}^{\int_0^Z G(Z')\,\mathrm{d}Z'} - R^2K(Z,R,T)\Big]F(\theta) = 0. \tag{10}$$

It is noted that the first three terms on the left-hand side of Eq. (10) are all functions of θ, the terms in the square bracket are functions of ϕ and T, therefore optical lattice potential $K(Z,R,T) = |F(\theta)|^2\,\Pi_n^2\exp(\int_0^Z G(Z')\,\mathrm{d}Z')/(1-2Z)^2$ can be obtained. Hence we obtain the Bessel equation with a variable parameter λ as

$$\frac{\mathrm{d}^2F(\theta)}{\mathrm{d}\theta^2} + \frac{1}{\theta}\frac{\mathrm{d}F(\theta)}{\mathrm{d}\theta} + \left(\lambda^2 - \frac{m^2}{\theta^2}\right)F(\theta) = 0. \tag{11}$$

Obviously, equation (11) has the Bessel function solution $F(\theta) = d_1\mathrm{J}_m(\lambda\theta) + d_2\mathrm{Y}_m(\lambda\theta)$, where $\mathrm{J}_m(\lambda\theta)$ and $\mathrm{Y}_m(\lambda\theta)$ are the Bessel functions of the first and the second kind, respectively.

When $R\to 0$, $F(\theta)$ should be finite, then $d_2=0$ is necessary. The resulting solution to Eq. (11) is expressed as $F(\theta) = d_1\mathrm{J}_m(\theta)$, where the Bessel polynomial has the form of

$$\mathrm{J}_m(\theta) = \sum_0^\infty (-1)^k\frac{1}{k!\Gamma(l+k+1)}\left(\frac{\theta}{2}\right)^{l+2k}.$$

Considering boundary condition $\Psi(R)|_{R=R_0} = 0$ and solving $\mathrm{J}_m(\lambda\theta) = 0$, we readily obtain eigenvalue $\lambda = \lambda_l^m = \mu_l^m/R_0$ and normalization constant $d_1 = \sqrt{2}/[R_0\mathrm{J}_{m+1}(\mu_l^m)]$, where l $(=1,2\ldots)$ is the quantum number, and μ_l^m corresponds to the l-th zero point of $\mathrm{J}_m(\lambda\theta)$. Hence, we can obtain the optical lattice potential as $K(Z,R,T) = \left|\mathrm{J}_m\left(\mu_l^m R/R_0\right)\Pi_n(T)\right|^2\exp[\int_0^Z G(Z')\mathrm{d}Z']/(1-2Z)^2$.

The final solution to Eq. (2) is given by

$$\Psi(Z,R,\phi,T) = \frac{d_1E_0}{1-2Z}\mathrm{J}_m\left(\frac{\mu_l^{(m)}}{R_0}R\right)\cdot\varphi_m(\phi) \times\Pi_n(T)\cdot\ \mathrm{e}^{\int_0^Z G(Z')\,\mathrm{d}Z' + \mathrm{i}\left[a+cR^2\right]}, \tag{12}$$

where correlative functions φ_m, Π_n, and a are given by Eqs. (7)–(9), respectively, and the chirp parameter is given by $c(Z,T) = c_0/(1-2c_0Z)$. The real envelope of the LB clusters in Eq. (12) is determined by degree (m,n) together with modulation depth q, lattice constant R_0, and energy $E(Z) = E_0\exp\left[\int_0^Z G(Z')\,\mathrm{d}Z'\right]$.

3. Form of the 3D LB cluster

In what follows, we present specific results of Eq. (12). The 3D Bessel–Hermite solution forms a cluster of LBs having some common characteristics. In Figs. 1 and 2, we present contour plots of spatiotemporal field distributions $|\Psi_{mn}|^2$ above a cutoff intensity through choosing the initial conditions and the parameters. The typical values are as follows: $a_0 = c_0 = 1$, $G(Z) = G_0 = R_0 = 6$, $E_0 = 2$, and $Z = 4$.

Figure 1 displays the structures and the distributions of the LBs for different values of m and n in the case of $q=0$. It is shown that there are $(n+1)$-layer ellipsoid solitons along the propagation direction (Z axis) and there are a set of different ellipsoid solitons in each layer. The distributions change regularly with the azimuthal angle. It is clearly seen that when $m\neq 0$, the LBs are a set of different ellipsoid solitons. However, when m is large enough, the ellipsoids form a necklace soliton ring with different radii sharing the same centre. The number of the ellipsoids in each ring is $2m$ in the horizontal direction. We can see that the

larger the parameter m, the larger the necklace radius. Hence, we can see that the characteristics of the structure and the distribution of the LBs are determined by spatiotemporal quantum numbers m and n.

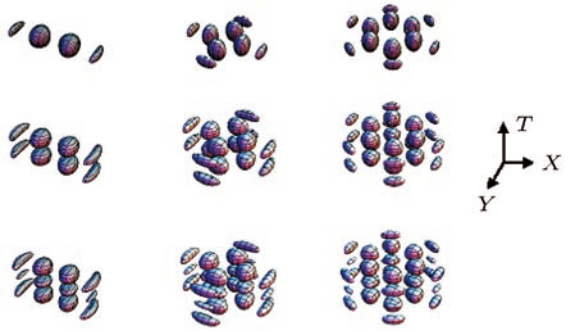


Fig. 1. (colour online) Structures and distributions of LBs for different values of m ($= 1, 2, 3$ from left to right) and n ($= 0, 1, 2$ from the first row to the third row), with selected parameters of $q = 0$, $a_0 = c_0 = 1$, $G(Z) = G_0 = R_0 = 6$, $E_0 = 2$, and $Z = 4$.

Figure 2 shows the structures and the distributions of the LBs for different values of m and n in the case of $q = 1$. It is shown that the distribution of the solitons has nothing to do with the azimuthal angle, which is consistent with Eq. (12). When $m \neq 0$, the intensity at the centre is zero. Moreover, it is found that the soliton profiles are self-similar and the radius of the wave packet becomes larger as m increases. The LB solitons form a family of vortex solitons with dark central intensities. As can also be seen from Fig. 2, the vortex solitons are transversely compressed, and the energy or the power of the wave packet becomes more concentrated as quantum number n increases. We summarize that in the limit of $q = 1$, the solitons exhibit the vortex shape with a radial symmetry, and the distribution of the LB solitons does not depend on the azimuthal angle.

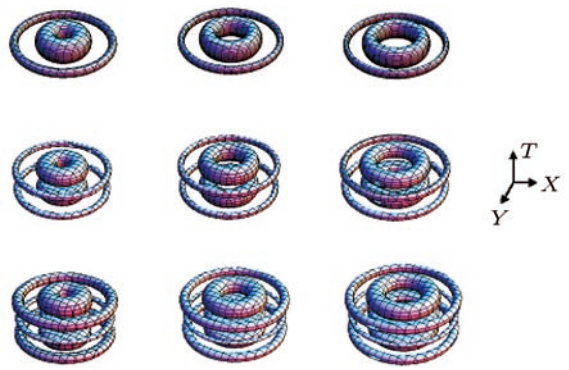


Fig. 2. (colour online) Structures and distributions of LBs with $q = 1$ for different values of m ($= 1, 2, 3$ from left to right) and n ($= 0, 1, 2$ from the first to the third row). Other parameters are the same as those in Fig. 1.

In Figs. 3 and 4, the expected analytical properties based on Eq. (12) have been confirmed by using the result obtained by the direct numerical integration of Eq. (2). In Fig. 3, we use a 3D split-step Fourier technique and consider the initial 3D field

$$|\Psi(0, R, \phi, T)|^2 = \left| E_0' J_2 \left(\frac{\mu_1^2}{R_0} R \right) \varphi_2(\phi) \cdot \Pi_0(T) \right|^2$$

from Eq. (12) for different distances ($Z = 2, 3, 6$) in the case of $m = 2$, $q = n = 0$, and $l = 1$. Here we set normalized energy parameter $E_0 = 1.97$ and gain $G_0 = 6$. The parameters correspond to those of the input pulses of millimeter-scale diameter, microjoule energy and a gain of ~ 8 dB over a diffraction length.[32] In order to confirm the stability, we simulate the evolution of the input pulse or the input beam with a white noise of variance $\delta = 0.05$. It is shown that the white noise does not change the self-similar characteristic of the soliton solution. As expected, the collapse is invisible. Our analytical solution (12) is in excellent agreement with the numerical simulation.

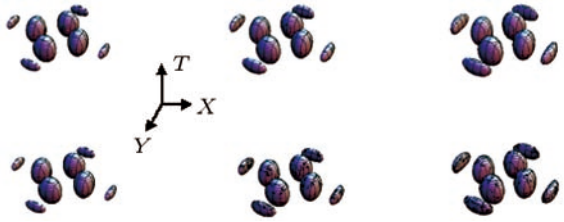


Fig. 3. (colour online) Distribution comparisons of the analytical solution with the numerical simulation for various distances ($Z = 2, 3, 6$ from left to right). The top row gives the analytical solution, the bottom row gives the numerical simulation with a white noise of variance $\delta = 0.05$. Some parameters are $n = q = 0$ and $m = 2$. The other parameters are the same as those in Fig. 1.

Moreover, figures 4(a) and 4(b) show the transverse phase and the amplitude distribution of the LBs at $Z = 2$. Here the chirp parameter is given by $c(Z, T) = c_0/(1 - 2c_0 Z)$, with $\Omega_i = -\partial\Phi/\partial R_i = -2c_0 R_i/(1 - 2c_0 z)$ ($R_i = X, Y$) denoting the chirps along the two transverse axes. It is shown that the quadratic phase structure in Fig. 4(a) and the vortex torus shape in Fig. 4(b) are particularly apparent. We stress that although the pulse expands in both spatial and temporal dimensions, it nonetheless remains spatiotemporally bound, representing a class of fantastic light bullet. The spatiotemporal localization is shown explicitly in the isosurface distributions given in Figs. 1 and 2. Figures 4(c) and 4(d) show the simulated chirp and the simulated intensity of the LBs with

$m = 2$ and $n = 1$ compared with the analytical predictions, respectively. It is noted that the chirp varies linearly with Z. We have also performed numerical simulations to demonstrate the stability of those linearly chirped pulses by adding a white noise $\delta = 0.05$ and by evolving from an initial chirped spatiotemporal soliton pulse of Eq. (12)

$$\Psi(0, R, \phi, T) = E_0 \mathrm{J}_2\left(\frac{\mu_1^2}{R_0} R\right) \cdot \varphi_2(\phi) \cdot \Pi_1(T) \cdot \mathrm{e}^{\mathrm{i}\left(a + cR^2\right)}$$

with $m = 2$ and $n = l = 1$. It is found that the chirped pulse and the chirped intensity are rather stable and propagate self-similarly.

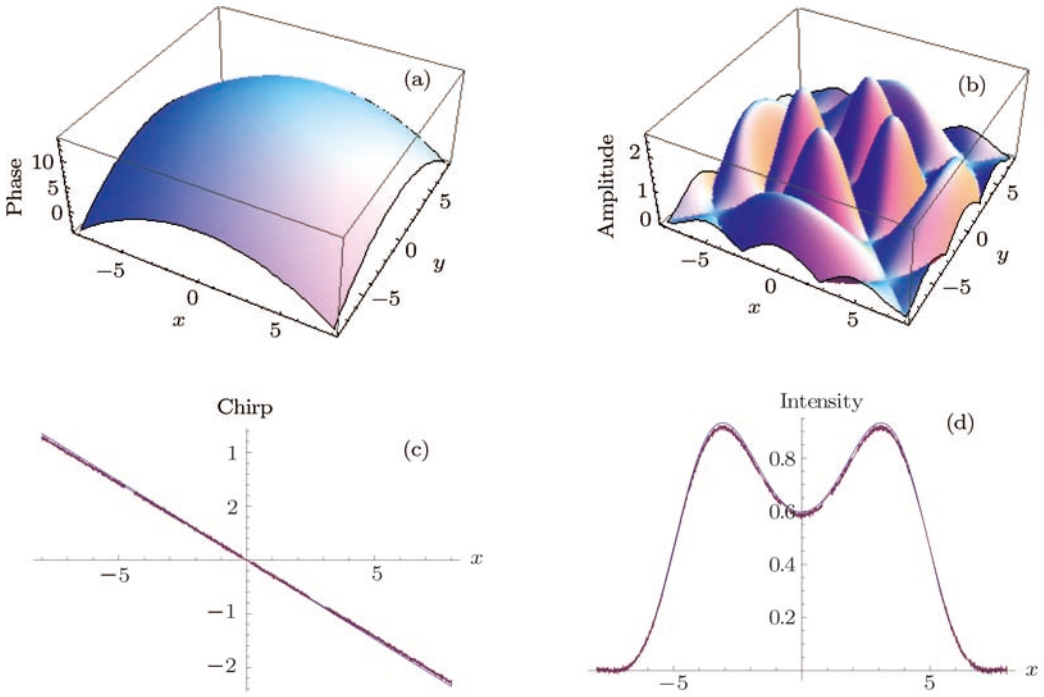


Fig. 4. (colour online) Self-similar LBs with $m = 2$ and $n = 1$ at $Z = 2$. Panels (a) and (b) show transverse phase Φ and amplitude distributions $|\Psi|$, respectively. Panels (c) and (d) show simulated chirp Ω_i $(i = X, Y)$ and intensity $|\Psi|^2$ (solid line) compared with the analytical predictions (dashed line). Other parameters are the same as those in Fig. 1.

4. Conclusion

We find an analytical solution of self-similar waves and Hermite–Bessel light bullets emerging in a three-dimensional nonlinear medium. The theoretical analysis and the numerical simulation show that the LBs are described by the Hermite and the Bessel functions in cylindrical coordinates and each of them attains a shape of the ellipsoid or the ring according to the modulation depth of the spatiotemporal intensity distribution, forming a new family of LB. The unique properties of those solitons are also discussed in detail.

References

[1] Silberberg Y 1990 *Opt. Lett.* **15** 1282
[2] Hong Y and Yi T 2008 *Chin. Phys.* B **17** 1008
[3] Kivshar Y S and Agrawal G P 2003 *Optical Solitons: From Fibers to Photonic Crystals* (San Diego: Academic)
[4] Towers I N, Malomed B A and Wise F W 2003 *Phys. Rev. Lett.* **90** 123902
[5] Mihalache D, Mazilu D, Crasovan L C, Towers I, Buryak A V, Malomed B A, Torner L, Torres J P and Lederer F 2002 *Phys. Rev. Lett.* **88** 073902
[6] Fermann M E, Kruglov V I, Thomsen B C, Dudley J M and Harvey J D 2000 *Phys. Rev. Lett.* **84** 6010
[7] Dudley J M, Finot C, Richardson D J and Millot G 2007 *Nat. Phys.* **3** 597
[8] Ponomarenk S A and Agrawal G P 2006 *Phys. Rev. Lett.* **97** 013901
[9] Zhang P J, Hong Y and Yi T 2009 *Chin. Phys.* B **18** 2364
[10] Gaeta A L 2003 *Science* **301** 61
[11] Xu S L, Liang J C and Yi L 2010 *J. Opt. Soc. Am.* B **27** 99
[12] Yanga Z Y, Zhao L C, Zhanga T, Lia Y H and Yue R H 2010 *Opt. Express* **283** 3768
[13] Bergé L, Skupin S, Nuter R, Kasparian J and Wolf J P 2007 *Rep. Prog. Phys.* **70** 1633

[14] Baizakov B B, Malomed B A and Salerno M 2004 *Phys. Rev.* A **70** 053613

[15] Matuszewski M, Garanovich I L and Sukhorukov A A 2010 *Phys. Rev.* A **81** 043833

[16] Hoq Q E, Kevrekidis P G, Frantzeskakisc D J and Malomed B A 2005 *Phys. Lett.* A **34** 145

[17] Morandotti R, Peschel U and Aitchison J S 1999 *Phys. Rev. Lett.* **83** 2726

[18] Zhang X P 2011 *Acta Phys. Sin.* **60** 293 (in Chinese)

[19] Xu S L, Liang J C and Yi L 2010 2011 *Acta Phys. Sin.* **59** 138 (in Chinese)

[20] Fleischer J W, Segev M, Efremidis N K and Christodoulides D N 2004 *Phys. Rev. Lett.* **92** 123904

[21] Lin K Y and Chang S J 1988 *J. Phys.* A: *Math. Gen.* **21** 2635

[22] Arlt J and Dholakia K 2000 *Opt. Commun.* **177** 297

[23] Vasara A, Truunen J and Fribert A 1989 *J. Opt. Soc. Am.* A **6** 1748

[24] Kartashov Y V, Vysloukh V A and Torner L 2005 *Phys. Rev. Lett.* **94** 043902

[25] Kartashov Y V, Carretero-González R, Malomed B A, Vysloukh V A and Torner L 2005 *Opt. Express* **13** 10703

[26] Liang J C, Cai Z B, Yi L and Wang H C 2010 *Opt. Commun.* **283** 386

[27] Liang J C, Xu B and Cai Z B 2011 *J. Opt. Soc. Am.* B **28** 93

[28] Kartashov Y V, Vysloukh V A and Torner L 2004 *Phys. Rev. Lett.* **93** 093904

[29] Yang J, Musslimani Z H and Ziad H 2003 *Opt. Lett.* **28** 2094

[30] Mihalache D, Mazilu D, Lederer F, Malomed B A, Kartashov Y V, Crasovan L C and Torner L 2005 *Phys. Rev. Lett.* **95** 023902

[31] Buryak A V, Trapani P Di, Skryabin D and Trillo S 2002 *Phys. Rep.* 370 63

[32] Chen S H and Dudley J M 2009 *Phys. Rev. Lett.* **92** 233903